Comparison of the impact of preservation methods on amniotic membrane properties for tissue engineering applications

Mathilde Fenelon, Delphine B Maurel, Robin Siadous, Agathe Gremare, Samantha Delmond, Marlène Durand, Stéphanie Brun, Sylvain Catros, Florelle Gindraux, Nicolas L'Heureux, et al.

Title: **Comparison of the impact of preservation methods on amniotic membrane properties for tissue engineering applications.**

Mathilde Fenelon*[1,2], Delphine Maurel[1], Robin Siadous[1], Agathe Gremare[1], Samantha Delmond[3,4], Marlène Durand[1,3,4], Stéphanie Brun[5], Sylvain Catros[1,2], Florelle Gindraux[6,7], Nicolas L'Heureux[1], Jean-Christophe Fricain[1,2]

[1] Univ. Bordeaux, INSERM, Laboratory BioTis, UMR 1026, F-33076 Bordeaux, France

[2] CHU Bordeaux, Department of Oral Surgery, F-33076 Bordeaux, France

[3] CHU Bordeaux, CIC 1401, 33000, Bordeaux, France

[4] Inserm, CIC 1401, 33000 Bordeaux, France

[5] University hospital, Gynecology-Obstetrics Service, F-33076, Bordeaux, France

[6] Orthopedic, Traumatology & Plastic Surgery Department - University Hospital of Besançon, Besançon, France

[7] Nanomedicine Lab, Imagery and Therapeutics (EA 4662) - SFR FED 4234 - University of Franche-Comté - Besançon, France

*Corresponding author

mathilde.fenelon@u-bordeaux.fr

ABSTRACT

Human amniotic membrane (hAM) is considered as an attractive biological scaffold for tissue engineering. For this application, hAM has been mainly processed using cryopreservation, lyophilization and/or decellularization. However, no study has formally compared the influence of these treatments on hAM properties. The aim of this study was to develop a new decellularization-preservation process of hAM, and to compare it with other conventional treatments (fresh, cryopreserved and lyophilized).

The hAM was decellularized (D-hAM) using an enzymatic method followed by a detergent decellularization method, and was then lyophilized and gamma-sterilized. Decellularization was assessed using DNA staining and quantification. D-hAM was compared to fresh (F-hAM), cryopreserved (C-hAM) and lyophilized/gamma-sterilized (L-hAM) hAM. Their cytotoxicity on human bone marrow mesenchymal stem cells (hBMSCs) and their biocompatibility in a rat subcutaneous model were also evaluated.

The protocol was effective as judged by the absence of nuclei staining and the residual DNA lower than 50 ng/mg. Histological staining showed a disruption of the D-hAM architecture, and its thickness was 84% lower than fresh hAM ($p < 0.001$). Despite this, the labeling of type IV and type V collagen, elastin and laminin were preserved on D-hAM. Maximal force before rupture of D-hAM was 92 % higher than C-hAM and L-hAM ($p<0.01$), and D-hAM was 37 % more stretchable than F-hAM ($p<0.05$). None of the four hAM were cytotoxic, and D-hAM was the most suitable scaffold for hBMSCs proliferation. Finally, D-hAM was well integrated *in vivo*.

In conclusion, this new hAM decellularization process appears promising for tissue engineering applications.

Key words: Amniotic membrane; *in vivo* Biocompatibility; Cryopreservation; Freeze-drying; Acellular scaffold; Processed amnion; Rat

I- Introduction

The human amniotic membrane (hAM) is the innermost layer of the fetal membrane and is in contact with the amniotic fluid. It contains three layers: an epithelial layer, a mesenchymal layer also known as the stromal layer, and a basement membrane, which separates them. Its thickness ranges from 20 to 500 µm [1]. The epithelial layer contains a single layer of human amniotic epithelial cells (hAECs) with a columnar or cuboidal shape [2]. The epithelium lies on a basement membrane containing mostly type IV collagen and laminin. The latter play a key role in the attachment of epithelial cells and in the cellular proliferation, migration and differentiation of hAECs [3]. Fibronectin, another component of the basal membrane, is also found in the stroma layer [3]. The amniotic stroma is comprised of three layers from inside to outside: an inner compact layer, a fibroblast layer and a spongy layer [1,2]. The stromal extracellular matrix mainly contains collagen type I, III, V, VI, laminin and fibronectin [4]. This membrane is neither vascularized nor innervated so it is a translucent biological structure.

Because it is considered as surgical waste after delivery, hAM is easy to procure and is widely available. Since its first clinical use for skin replacement in 1910 by Davis, hAM is routinely used in ophthalmology and dermatology and remains the gold standard substrate for the ex vivo expansion of human limbal stem cells to treat corneal blindness [5–8]. hAM contains immunoregulatory factors such as HLA-G and Fas ligand, which have been linked to its low immunogenicity [9–11]. hAM is also known to display an anti-inflammatory and antifibrotic effect and to enhance wound healing [12–16].

Thanks to these biological properties, the low cost of harvesting and good clinical outcomes, hAM has become a highly attractive and promising scaffold for tissue engineering. Several studies have used hAM as a biological scaffold upon which different cell types can grow and differentiate [17–19]. To allow prolonged storage, several preservation methods of hAM have been developed in order to prepare hAM prior to cell seeding for tissue engineering [6,20–22]. Cryopreservation and lyophilization are the techniques which are the most commonly used [23,24]. However, cryopreservation leads to very poor cell viability in hAM [25,26]. Therefore, to avoid implanting a tissue whose cell viability is not controlled, the decellularization of hAM emerged. Preserved hAM can thus be used directly or decellularized, i.e. without hAECs and human amniotic mesenchymal stromal cells (hAMSCs).

Various attempts have been made to decellularize hAM and they usually require two steps. First, hAM is exposed to chemical or enzymatic agents, then mechanical scraping is performed to remove the loosened cells [21,27–31]. This adjunctive scraping step requires the removal of residual cells under light microscopy, so the procedure is operator-dependent. Furthermore, mechanical scraping may cause severe damage to the basement membrane integrity [32,33]. Only a few studies have suggested new decellularization methods that do not require additional mechanical scraping [16,34–38]. Despite favorable reports, the techniques proposed are very time-consuming since they last several days. Whatever the treatment used (cryopreservation, lyophilization, decellularization or gamma-sterilization), they all have some limitations because the processing and preservation of hAM affect its properties [6,39]. The composition or the distribution of the extracellular matrix and basement membrane components of hAM is often affected by preservation [23,30,40]. It has also been shown that the preservation of hAM decreases the amount of growth factors [40,41], and leads to changes in its physical and mechanical properties [23,39,42]. However, few studies have compared the properties of these different hAM with fresh hAM for tissue engineering applications, and there is still no consensus about the optimal method for preserving hAM prior to its use as a scaffold for tissue engineering.

The objective of this study was first to develop a simple and reproducible method for the effective decellularization and preservation of hAM. We also aimed to establish the most suitable preservation method based on morphological, biomechanical, histological, *in vitro* cytocompatibility and *in vivo* biocompatibility parameters.

II- Materials and Methods

• 2.1. Harvest and preservation methods of hAM

- Tissue collection

Eleven human placentas were collected after elective cesarean surgery from consenting healthy mothers (tested seronegative for HIV, cytomegalovirus, Toxoplasma gondii, Hepatitis B and C virus, and syphilis). Patients provided written informed consent as requested by the institutional review board and their placentas were anonymized. The placentas were kept in a sterile solution containing PBS 1x (Gibco®) supplemented with 1% antibiotics (penicillin/ streptomycin, Invitrogen®) to be transferred to the laboratory. Then, they were rinsed with sterile distilled water and residual blood clots were removed. The amniotic membrane was

peeled from the chorion and rinsed with sterile distilled water again before storing. All these steps were performed under sterile conditions.

- Preparation and storage of hAMs

Four treatments of hAM were performed in this study: fresh (F-hAM), cryopreserved (C-hAM), lyophilized (L-hAM) or decellularized then lyophilized hAM (D-hAM). All steps were done under aseptic condition. Fresh hAM (F-hAM) was kept in plates containing α-minimum essential medium (MEM alpha, GIBCO®), 10% fetal bovine serum (FBS, Eurobio®) and 1% antibiotics (amoxicillin/ streptomycin Invitrogen®). It was stored in this medium in an incubator (37°C, 5% CO_2, 100% humidity) for a maximum of two days before use. For C-hAM, pieces of hAM were put in a solution of RPMI/glycerol 1:1 and kept frozen at -80°C. When needed, C-hAM was thawed and washed twice with sterile PBS 1x before further analysis. To prepare L-hAM, patches were frozen at -80°C, then dried under vacuum in a freeze dryer. For D-hAM, hAM was first treated with trypsin and ethylenediaminetetraacetic acid (T/EDTA, 0.125%) for two minutes at 37°C. It was washed with sterile PBS for 15 min, transferred to a decellularization solution composed of 8 mM CHAPS, 25 mM EDTA, 0.12 M NaOH and 1 M NaCl in PBS and then incubated under gentle agitation for 7h at room temperature. Following this treatment, hAM was washed thoroughly overnight in three changes of sterile distilled water with vigorous shaking. Finally, D-hAM was frozen at -80°C, before being dried in the freeze dryer. L-hAM and D-hAM were put in sterilization pouches before being sterilized by gamma radiation at 25 kGy (Gamacell® 3000 Elan, NORION MDS, Ottawa, Canada). They were stored in their sterilization pouches at room temperature and kept in the dark until analysis.

- Validation of decellularization method

To ensure the effectiveness of the decellularization process, we used previously established guidelines for decellularization [32]. D-hAM was compared to non-treated amnion using qualitative and quantitative criteria (n=3 for each experiment). First, DAPI staining was conducted to visualize the presence of any residual nuclei on D-hAM and non-decellularized hAM using confocal microscopy (Leica TCS SPE Model DMI 4000B). In addition, samples of hAM from the four groups were fixed in 4% paraformaldehyde (Antigenfix, Microm Microtech, France), dehydrated by baths of increasing ethanol concentrations and paraffin-embedded. Samples of fresh and preserved hAM were then sectioned with a microtome (7 µm) and stained with DAPI. Cross-sections were observed with the same confocal microscopy. In the second experiment, after freeze-drying and grinding hAM, residual DNA was extracted from D-hAM and non-treated hAM in order to be quantified with a DNA

extraction kit (QIAmp® DNA Mini Kit, Qiagen, USA) according to the manufacturer's instructions. DNA was then quantified with a spectrophotometer by determining its absorbance at 260/280 nm wavelength (*Implen* NanoPhotometer® P-Class P330). The value obtained (ng/µL) was plotted against the weight of the dry samples (ng/µg). Finally, to determine the size of the remaining DNA, equal concentrations of extracted DNA from non-treated and decellularized hAM were separated by agarose gel electrophoresis 1.5% and visualized with ultraviolet transillumination using a ladder (FastRuler low range DNA Ladder, Thermofisher®).

- **2.2. Characterization of fresh and preserved hAM**
  - Histological assessment

For histological analysis, samples of hAM from the four groups were fixed in 4% paraformaldehyde (Antigenfix, Microm Microtech, France), dehydrated by baths of increasing ethanol concentrations and paraffin-embedded. Samples of fresh and preserved hAM were then sectioned with a microtome (7 µm) and stained with hematoxylin and eosin saffron (HES). Images were obtained with an Eclipse 80i light microscope (Nikon, Japan) and captured with a DXM 1200C CCD camera (Nikon, Japan).

- Immunohistological study

To assess the effect of the preservation procedure, the distribution of 7 proteins of hAM extracellular matrix was assessed by immunohistochemistry. Sections of the paraffin-embedded samples were obtained with a microtome (5 µm), then glued with an albumin-glycerol mixture on treated slides. After dewaxing and rehydration of sections, a hyaluronidase pretreatment was performed. After washing in PBS, samples were incubated with the primary antibody overnight at 4°C to detect the presence of type I, III, IV, V collagen, elastin, laminin and fibronectin (See Supplementary Table S1). Having blocked endogenous peroxidase activity with 0.5% hydrogen peroxide, samples were incubated with the secondary antibody for 45 minutes at room temperature. Antigen-antibody complexes were revealed by tetrahydrochloride diaminobenzidine (DAB, Dako, K3468) and cells were slightly counterstained with Mayer's hematoxylin. Sections were mounted with aqueous medium for microscope observation.

- Biomechanical behavior

The physical and biomechanical properties of F-hAM, C-hAM, L-hAM and D-hAM were investigated. Briefly, the average thickness of fresh and preserved hAM was assessed with a laser sensor (Aeroel®, XLS 13XY XACTUM^{TM}). Uniaxial tensile tests were performed by using an Autograph tensile tester AGS-X (Shimadzu®). hAM samples were designed by using a dog-bone shaped punch similar to the ASTM D-638 type V (width: max= 7.5 mm, min= 2.5mm; linear length = 6mm; overall length= 38.63 mm). They were pre-tested at 20 mm/min until 0.1 N and stretched at a speed of 1% of loaded initial length (L_0) per second (typically around 0.24 mm/s). The samples remained wet during the mechanical testing. If failure did not occur in the center of the sample, the sample was discarded. Maximal force before rupture (Fmax) and strain at failure (Smax) were recorded using Trapezium X® software.

- **2.3. *In vitro* cytocompatibility studies**

Human bone marrow mesenchymal stem cells (hBMSCs) were utilized for the cytocompatibility studies. The hBMSCs were isolated from consenting patients who had undergone hip surgery (experimental agreement with *CHU de Bordeaux* and *Etablissement Français du Sang*, agreement CPIS 14.14), and expanded according to well-established protocols [43]. Cells were used at passage 1 for this study.

- Extract cytotoxicity assay

First, we wanted to assess the cytotoxicity of the preservation method. For this purpose, the cytotoxicity of soluble extracts obtained from the four membranes (F-hAM, C-hAM, L-hAM and D-hAM) was evaluated according to the NF-EN-ISO 10993-5 standards by measuring the cell viability and the metabolic activity of hBMSC using a neutral red assay and a 3-(4-5 dimethylthiasol-2-yl) diphenyl tetrazolium (MTT) assay, respectively. For both studies, cell culture medium extracts were prepared according to the EN 30993-5 European standard. Pieces of the four hAMs (n=12 for each preservation method) were put in 24-well plates containing 400 µl of α-minimum essential medium (MEM alpha, GIBCO®), 1% antibiotics (Invitrogen®), then incubated at 37°C in a humidified atmosphere containing 5% CO_2 in air. The medium extracts were collected after 24 h (E1) and replaced by the same volumes of medium. Medium extracts were stored at -20°C. The procedure was repeated every day for three days (E2 and E3). For both Neutral Red and MTT assays, hBMSCs were plated at

$1.5x10^4$ cells/cm^2 in 96-well plates and cultured for 72 hours to reach cell confluence. After removal of culture media, soluble extracts (E1, E2 and E3) of the four hAMs supplemented with 10% FBS were added and incubated for 24 hours. Triton 100X at 0.1% was used as a negative control and α-MEM culture medium alone was used as a positive control.

To assess the effect of hAM soluble extracts on the cell viability of hBMSCs, the culture medium was removed after 24 hours of contact with soluble extracts, and a solution of 100 µl of Neutral Red (Sigma-Aldrich Co), diluted in 1.25% IMDM supplemented with 10% FBS, was added to each well and cultured at 37 °C, 5% CO_2 for 3 hours. Then, the supernatant was removed and 100 µl of a solution made of 1% acetic acid in 50% ethanol were added to lyse the cells. Staining intensity was quantified by measuring the absorbances at 540 nm with a spectrophotometer (Perkin Elmer®, 2030 Multilabel Reader Victor™X3).

To assess the metabolic activity, the culture medium was removed after 24 hours of contact and replaced with 125 µl solution of MTT (Sigma-Aldrich Co, 5 mg/ml in 0.1 M PBS, pH = 7.4), which was diluted (20% in IMDM without phenol red (Gibco®) and cultured for 3 hours at 37°C, 5% CO_2 to form blue formazan crystals. Subsequently, the supernatant was removed and 100 µl of dimethyl sulfoxide (DMSO; Sigma-Aldrich Co) were added to the plates to dissolve the formazan crystals. Staining intensity was quantified by measuring the absorbance at 570 nm with a spectrophotometer (Perkin Elmer®, 2030 Multilabel Reader Victor™X3). For both assays, the results of each condition were normalized to positive controls (cells cultured on plain plastic surfaces in basal medium) for each incubation time (as 100% cell viability and metabolic activity).

- Contact cytotoxic assay

We aimed to compare the suitability of fresh and preserved hAM to be used as a scaffold upon which hBMSCs can adhere and growth. Thus, the metabolic activity of hBMSCs cultured over fresh and preserved hAM was evaluated at 1, 3 and 10 days post-seeding by using a resazurin-based assay [44,45]. Metabolic activity of hBMSCs cultured in 2D conditions on tissue culture polystyrene (TCPS) plates served as a positive control. Briefly, samples of hAM were cut into circles, put in 24-well plates and maintained in place with home-made rings (n=9 for each condition). hBMSCs were seeded on each sample at a density of $2.5x10^4$ cells per well and cultured for 10 days. An alamar blue assay was performed on day 1, 3, 7 and 10. Briefly, a solution of resazurin (0.1 mg/ml in PBS) was added to each well to a final 10% (v/v) concentration. After 3 h incubation at 37°C, 200 µl of the medium were transferred to a 96-well plate and measured by fluorescence (exc. = 530 nm, em. = 590 nm,

Victor X3, Perkin Elmer). Results were expressed as percentage of metabolic activity of cells relative to 2D conditions at day 1.

- **2.4. *In vivo* biocompatibility**

  - Subcutaneous implantation

The present study was approved by the French Ethics Committee (agreement APAFIS n°4375-2016030408537165v8). Thirty 10-week-old female Wistar rats were used. The biocompatibility of the four hAM was assessed using a rat subcutaneous implant model. The aim was to implant patches of F-hAM, C-hAM, L-hAM and D-hAM (10 x 10 mm) in the dorsal subcutaneous tissue of adult rats and to compare their biocompatibility. As hAM is a resorbable material, we used blue non-absorbable sutures (Prolene™ Visi-Black™ 6-0, Ethicon®) to fix it at each of the four corners of the samples and to act as a marker for identifying the implantation sites. Surgery was carried out under aseptic conditions. Short-term anesthesia was induced by inhalation of 4% isoflurane (Air:1.5 L/min) and maintained using isoflurane 2% (Air: 0.4 L/min). Analgesia was performed by intraperitoneal injection of 0.1 mg/kg buprenorphine (Buprecare®, 0.3 mg/ ml). The back was shaved, the surgical site was aseptically prepared, and a midsagittal incision was made in the back area. Three conditions were implanted on either side of the mid-dorsal line (n=6 conditions per rat). In addition to the four implanted hAM, two negative controls were performed for this study: a sham-operated control with no biomaterial implantation (sham) and a negative control for which only non-absorbable sutures were made (suture). Implants were spaced at least 10 mm apart, and each implant base was more than 10 mm from the line of incision. After surgery, food and water were supplied *ad libitum*. Euthanasia was performed one week, one month and two months after implantation using CO_2 inhalation (n=30 rats; 10 rats per time point). After shaving, the samples were carefully harvested and rinsed with PBS 1x, then placed in 4% paraformaldehyde (Antigenfix, Microm Microtech, France) overnight. Then, the 180 explanted samples were rinsed in PBS 1x and processed for histology and immunofluorescence.

  - Histological and immunolabeling analysis of implants

Samples were dehydrated and processed for conventional embedding in paraffin. Seven-µm-thick serial sections were made. First, immunolabeling of type I collagen was performed in order to reveal the presence of residual hAM (Abcam, ab34710). Briefly, deparaffinized

sections were pretreated with citrate (pH 6.0) for 20 min at 95°C and were then washed with PBS. To block non-specific binding sites, 5% BSA (bovine serum albumin) in PBS was used for 30 min at room temperature. Anti-collagen I antibody diluted in 5% BSA in PBS (1:200) was applied on sections overnight at 4°C. Secondary antibody Alexa Fluor 568-conjugated goat anti-rabbit (Invitrogen, A11036) was diluted (1:300) and applied for 1h30 at room temperature in the dark. Cross-sections of the suture control samples were used as control.
Then, the 180 samples were stained with HES and images were acquired with a slide scanner (Hamamatsu Nanozoomer 2.0HT). The resorption of hAM patches over time and for each condition was measured on HES staining using NDPview software (one section per sample) by two investigators. The dimension of residual hAM calculated on the stained section was plotted against the initial dimension of the implants. Finally, according to the NF-EN-ISO 10993-6 standard, a blinded independent trained investigator scored the inflammatory reaction around the implants semi-quantitatively by HES staining. The following biological response parameters were assessed and recorded: cellular infiltration and inflammatory cell type (polymorphonuclear, lymphocytes, macrophages, plasma cells and giant cells), vascularization, fatty infiltration and extent of fibrosis. The scoring system was as follows: the test sample was considered as non-irritant (0.0 up to 2,9), slightly irritant (3.0 up to 8.9), moderately irritant (9.0 up to 15.0) or severely irritant (> 15) to the tissue as compared to the sham-operated control sample.

- **2.5. Statistical analysis**

Results are expressed as mean ± standard deviation, with n indicating the number of hAM samples tested. Statistical analysis was performed using GraphPad Prism Software (La Jolla/CA, USA). First, a normality test was performed using a D'Agostino and Pearson omnibus normality test. If data assumed Gaussian distribution, differences were assessed by one-way analysis of variance (ANOVA) with the Bonferroni post-test, whereas statistical significance for independent samples was evaluated with the non-parametric Kruskal-Wallis test followed by Dunn's multiple comparison test. In both cases, statistical significances are marked by stars with * indicating a two-tailed $p < 0.05$, ** $p < 0.01$, and *** $p < 0.001$.

III- Results

- **3.1. Decellularization: DAPI staining DNA quantification and agarose gel electrophoresis assessment**

No positive staining was observed after the decellularization process, demonstrating the absence of residual nuclei (Fig 1A and B). This result was confirmed by DNA quantification. The amount of residual DNA in D-hAM was lower than 50 ng/mg of dry tissue (remaining DNA of non-treated hAM and D-hAM: 5408 ± 3341 and 42 ± 12 ng/mg respectively, $p<0.05$) (Fig 1C). Furthermore, no residual DNA was visible in the decellularized tissue gel electrophoresis after the decellularization process (Fig 1D).

- **3.2. Morphological aspect, ECM composition and mechanical properties of fresh and preserved hAM**

The morphology of fresh and preserved hAM was assessed by HES staining (Fig 2A). The organization of the epithelium was maintained as a single layer of columnar or cuboidal cells in F-hAM, C-hAM and L-hAM, whereas the complete lack of residual cells was obvious after decellularization. This result supported the validation of the decellularization process of D-hAM. The epithelial cells were slightly damaged by cryopreservation and lyophilization and vacuolar degeneration was observed in C-hAM and L-hAM. The trilaminar architecture of hAM (epithelium, basement membrane and mesenchymal layer) was preserved in F-hAM. The epithelial and the mesenchymal layers could be identified in C-hAM and L-hAM, whereas the architecture was no longer observable in D-hAM. The stroma layer remained unchanged after cryopreservation, although it was much thinner and denser in L-hAM and D-hAM.

Immunohistochemistry was also performed to investigate whether the extracellular matrix and basement membrane proteins remained unchanged after the treatments (Fig 2B). Before treatment, F-hAM was distinctly labeled for type I, III, IV and V collagen, elastin, fibronectin and laminin in the basement membrane and stromal layer. After cryopreservation, the architecture of the amnion seemed unchanged. However, type IV collagen and laminin labeling were slightly decreased by the treatment. After lyophilization, we observed a labeling of type I, IV and V collagen, elastin, fibronectin and laminin, whereas the labeling of type III collagen was reduced or absent. The other labeling persisted in D-hAM except for type I, type III collagen and fibronectin labeling, which were absent or greatly reduced.

Finally, to compare the physical and mechanical properties of hAM, the thickness, maximal force (FMax) and strain at failure (SMax) of fresh and preserved hAM were assessed. L-hAM and D-hAM were significantly thinner than F-hAM. C-hAM appeared thicker than F-hAM,

but no statistical difference was observed (Fig 3A). D-hAM was significantly stronger than C-hAM and L-hAM ($p<0.001$). Furthermore, no statistical difference in FMax was observed between F-hAM and D-hAM, suggesting that this treatment did not compromise the mechanical properties of hAM (Fig 3B). D-hAM was also significantly more stretchable than F-hAM (Fig 3C).

- **3.3. *In vitro* cellular response**

Cell viability was evaluated with red neutral assay. There was a significant reduction in the viability of hBMSCs when they were cultured with the first soluble tissue extract of C-hAM (Fig 4A). No decrease in cell viability was observed with the second and third extracts. The metabolic activity of hBMSCs was evaluated by the MTT test. The first extracts from C-hAM also significantly reduced the metabolic activity of hBMSCs and this reduced activity was also observed with the third extract (Fig 4B). However, since the cell viability and metabolic activity of hBMSCs were always higher than 70 %, the four hAM may be considered non-cytotoxic according to NF-EN-ISO 10993-5 standards.

We also assessed the capacity of hBMSCs to attach and proliferate over fresh and preserved hAM. At day 1, the metabolic activity of hBMSCs seeded on any hAM was significantly higher than that of hBMSCs cultured on plastic. At subsequent time points, metabolic activity was significantly enhanced compared to control (hBMSCs cultured on plastic) only when cells were seeded over D-hAM (Fig 4C).

- **3.4. *In vivo* biocompatibility**

All implants could be sutured to the subcutaneous tissue of rats during surgery (Fig 5). However, L-hAM and D-hAM were easier to handle and to suture than F-hAM and C-hAM. They were stiffer, more resistant to tearing and did not fold. As non-absorbable sutures were used to mark the implantation site, all the 174 samples could be easily located one week, one month or two months after surgery (n=10 per time point for each condition, except at one week since one rat died during surgery, so n=9).

- Resorption of hAM

First, the immunofluorescence staining of type I collagen showed the presence of F-hAM and C-hAM one week after surgery, whereas no staining was evidenced thereafter in these membranes (Fig 6A). Staining of L-hAM was no longer visible two months after surgery and

D-hAM was the only condition in which type I collagen staining was still present two months after surgery (Fig 6A).

Then, these data were corroborated by measuring the resorption rate of fresh and preserved hAM by histological analysis (Fig 6A and B). One week after surgery, the degradation of fresh and preserved hAM had already started. D-hAM had the lowest resorption rate but there was no significant difference between the four membranes at one week. One month after surgery, F-hAM and C-hAM were almost fully resorbed. L-hAM seemed to have degraded faster than D-hAM after one week and one month, but the difference became statistically significant only after two months. Thus, D-hAM had the slowest rate of resorption since it was the only membrane that was still present two months after implantation.

- Inflammatory reaction

To evaluate the host response, a blinded independent trained investigator scored the inflammatory reaction around the implants semi-quantitatively by HES staining (Fig 7A and 7B). Values were expressed as the difference between the test sample (hAM and non-absorbable suture control) and the control sample (sham-operated control).

One week after surgery, a slight inflammatory reaction was observed around fresh and preserved hAM compared to the sham-operated control. The acute inflammatory reaction was clearly visible around F-hAM and C-hAM implants, with cells penetrating the implant (Fig 7A). L-hAM and D-hAM caused less inflammation and no host cell infiltration was observed in the implant (Fig 7A). One month after surgery, L-hAM and D-hAM had induced a higher cellular response than F-hAM and C-hAM, which were completely degraded by then. Two months after surgery, the inflammatory reaction had abated in all the conditions. However, only D-hAM maintained a slight active inflammatory reaction, where host cell infiltration associated with delamination of D-hAM was observed (Fig 7A).

Based on ISO 10993-6:2007 scoring, fresh (F-hAM), preserved hAM (C-hAM, L-hAM and D-hAM) and suture controls were considered slightly-to-moderately irritant to the tissue as compared to the sham-operated control (Fig 7B). Similar results were obtained with the suture control samples, which induced a slight inflammatory reaction compared to the sham samples too.

IV- Discussion

We developed and characterized a new acellular amnion-based scaffold suitable for tissue engineering, and compared it with all conventional methods to preserve hAM. Some hAM

decellularization processes have already been used to obtain an acellular amniotic membrane. Although they were successful in removing cells, they either required mechanical scraping [27–29], which induces variability, or involved multi-day treatments with enzymatic and/or harsh chemical agents [34–36,38,46]. Our new method is effective, not time-consuming and does not require mechanical scraping. First, to avoid exposing tissues to cell removal agents for long incubation times, we added a short incubation time with T/EDTA as a first step. For dense tissue, exposure to trypsin may be needed to improve the penetration of the decellularization agent and obtain a completely acellular scaffold [47]. Then, we used a decellularization method that has proved successful for decellularizing tissue-engineered vascular grafts [48]. There were no residual nuclei with DAPI staining and residual DNA was less than 50 ng/mg, which is considered as an acceptable threshold to avoid an adverse host response [32,49].

Cryopreservation and lyophilization are the most commonly used hAM preservation procedures [23]. Once the hAM was decellularized, we performed lyophilization and gamma sterilization prior to its use to allow long-term storage. Freeze-drying (i.e. lyophilization) allows the safe storage of samples for several years at room temperature [22,25,50], whereas cryopreservation requires expensive equipment that may be unavailable in some institutions, and the storage time cannot exceed 12 to 24 months [6,51]. Furthermore, the cold chain involves complex transportation procedures and the samples need to to be thawed before use [50,51]. Lyophilized hAM appears easier to store, and it is usually followed by sterilization of the amniotic tissue by gamma radiation [52]. Gamma radiation is used worldwide for sterilizing medical products, and it is considered the most reliable and effective method to sterilize tissue allografts [25].

Treatment of hAM raises issues regarding its biological and mechanical properties. Several studies have already reported some damage in the expression or the distribution of the extracellular matrix and basement membrane components of hAM after preservation [23,30,40]. In this study, the morphology of the hAM and the protein distribution were altered by the three preservation methods tested. Delamination of the stroma was also observed in D-hAM. This disruption is commonly induced by decellularization processes [30,40,53]. In our study, except for fibronectin, labeling of the other proteins was still observed after the decellularization of hAM, although it was sometimes slightly or highly reduced. In addition, our process did not damage the integrity of the basement membrane components. Indeed, type IV collagen and laminin, which are abundant in the basement membrane, were still expressed. This could be due to the zwitterionic detergent used in this study (i.e. CHAPS), which usually

preserves the ultrastructure better than ionic detergents [32]. Moreover, not having used mechanical scraping may have contributed to preserving the basement membrane integrity.

The preservation and sterilization of hAM may also affect its biophysical properties as allogenic grafts [39]. However, to our knowledge, no study has simultaneously compared the mechanical properties of fresh, cryopreserved, lyophilized/gamma-sterilized and decellularized/lyophilized/gamma-sterilized hAM. Preservation caused significant changes in the thickness of hAM: it was significantly reduced in L-hAM and D-hAM, whereas C-hAM seemed thicker than F-hAM. These results are consistent with previous studies in which cryopreservation led to the uptake of hydrophilic glycerol and water, thus resulting in the swelling of C-hAM, whereas freeze-drying resulted in the loss of liquid [23,39,54]. Because the thickness of hAM varies significantly between donors [55] and also depends on the preservation procedures used, we decided to assess the mechanical characteristics of hAM using thickness-independent parameters, as done previously [23]. The tensile Fmax of F-hAM was significantly higher than that of cryopreserved and lyophilized hAM (65 % higher, $p<0.01$), and the Fmax of D-hAM was also 92% higher than that of C-hAM and L-hAM. Similar results were obtained by Niknejad *et al.*, who found that both cryopreservation and lyophilization induced lower maximal loads to failure than with fresh hAM [23]. This could be due to the extracellular matrix alterations that they induce. Other authors compared the mechanical properties of hAM after lyophilization and after decellularization and lyophilization [29]. They found similar results between both membranes, whereas in our study D-hAM was stronger than L-hAM. This could be because, unlike them, we did not use scraping, thus avoiding mechanically damaging the membrane. Another study comparing the mechanical properties of fresh and decellularized hAM showed no statistical difference between them [37]. The membrane was decellularized without scraping, then sterilized by using paracetic acid [37]. We thus hypothesized that the decellularization process play a protective role that preserved the matrix from a decrease of its mechanical properties following cryopreservation/lyophilization. We hypothesize that the cell removal caused by the decellularization created space inside the matrix to allow ice crystals to form without damaging the collagen network. This would result in better preservation of mechanical properties. Another explanation could be that the decellularization process somehow induces the formation of smaller ice crystal. A 3D-analysis would be necessary to be able to link the collagen network structure of hAM to its mechanical properties. Interestingly, we also found no statistical difference in Fmax between D-hAM and F-hAM, and D-hAM appeared to be 37% more stretchable than F-hAM ($p<0.05$). Mechanical results showed that decellularization

did not decrease the overall strength of the tissue. In addition, it made hAM more rigid than F-hAM and C-hAM, resulting in a membrane easier to handle and to suture without tearing during *in vivo* experiments. Figueiredo *et al.* also reported that decellularization followed by gamma irradiation stiffened hAM tissues [38]. However, depending on the targeted application, it could be interesting to further enhance the thickness and mechanical properties of D-hAM, perhaps by designing a multi-layered D-hAM scaffold [36,56].

Several differentiated cells such as human keratinocytes [17], human oral mucosal epithelial cells, human chondrocytes [18] and smooth muscle cells [35,57] have been successfully seeded on acellular amnion scaffolds. However, fewer studies have investigated its potential as a matrix for growing stem cells, a cell source that could be more promising for tissue engineering [36] and especially for bone regeneration [56]. Here we assessed the cytotoxicity of fresh and preserved hAM and compared their ability to support the proliferation of hBMSCs. As shown here and by other groups [23,29], we observed that fresh and preserved hAM were non-cytotoxic. However, cryopreservation caused a significant reduction in cell viability and metabolic activity. These results are consistent with previous studies, likely for two reasons [19,58]. First, they may be due to the use of glycerol as a cryoprotectant. Shortt *et al.* found that glycerol impaired the ability of hAM to act as a substrate for cell seeding compared to hAM cryopreserved in Hank's Balanced Salt Solution without glycerol [19]. Glycerol is known to display a growth-inhibitory effect that is dose-dependent on various cell types [59,60]. It may be induced by osmotic pressure change leading to a stress to cells, because water moves faster across the cellular membrane than glycerol [61]. Another possible explanation for this significant reduction is that the presence of autolytic enzymes released by the cells dying in the amniotic membrane could decrease cell viability after the extract cytotoxicity assay [37]. This is supported by the very poor survival of amnion-derived cells previously observed after cryopreservation [26]. Finally, in the context of tissue-engineering applications, we assessed the capacity of hBMSCs to attach and proliferate over fresh and preserved hAM. Whatever the preservation method used, the metabolic activity of hBMSCs was significantly greater once seeded on hAM than cultured on plastic at day 1. Over time, D-hAM was the most suitable scaffold for hBMSCs proliferation, as demonstrated by a significant enhancement of their metabolic activity. These results are consistent with previous studies that reported the successful proliferation of human and rat BMSCs seeded on an acellular hAM [62] [29,56]. In our study, the best results were achieved with D-hAM. This could be due to the fact that the decellularization process led to exposure of the basement membrane of hAM, thereby promoting its ability to support cell adhesion and proliferation.

Our decellularization process did not damage the integrity of the basement membrane components, which is essential to promote cell seeding.

Finally, we compared the biocompatibility of fresh and preserved hAM using subcutaneous implants in rats. The host response to fresh or preserved hAM implantation has already been studied in immunocompetent rodents [29,34,63]. Indeed, hAM is an immune-privileged tissue that contains some immunoregulatory factors such as HLA-G and Fas ligand, and has a low-to-absent level of expression of HLA class I and II molecules [9,64]. These characteristics should thus avoid the rejection of hAM by an allograft or xenograft. hAM is a resorbable biological scaffold, so unlike other authors [29,34], we decided to stabilize it with non-absorbable sutures so as to easily identify the implant site after sacrifice. As described earlier and by other groups, we observed an early degradation of fresh and cryopreserved hAM once implanted [15,63]. Lyophilization and gamma sterilization especially after decellularization significantly prolonged graft survival. In some applications such as bone regeneration, which requires around three months, the longevity of hAM grafts might be a critical parameter for proper healing. In such cases, D-hAM appears to be the most suitable scaffold since it displays the slowest rate of resorption. Another way to enhance their longevity would be to stack hAM to obtain multi-layered scaffolds [63]. We observed that fresh and preserved hAM are a biocompatible matrix, inducing a slight-to-moderate reaction as compared to the sham-operated control samples. However, the inflammatory reaction score for D-hAM was higher two months after surgery, probably because it was the only membrane still present two months after implantation. Furthermore, host cell infiltration of D-hAM occurred later, suggesting a protection effect against cellular infiltration like that offered by the barrier membrane used in clinical practice.

A limitation is that we did not assess the growth factor level of hAM as a function of the preservation method. Contradictory findings have been reported regarding the effect of preservation on the level of growth factors contained in hAM [22,25,41]. First, it could be because, depending on the targeted application, different growth factors were investigated, making the comparison between studies difficult. Second, preservation methods affect each growth factor differently. Third, a variation in growth factor content in amniotic membrane samples has been shown between donors, but it also depends on the region of the membrane and the delivery method [65,66]. In addition, several studies have reported successful scaffold function with preserved hAM despite their low concentration in growth factors [22,40].

CONCLUSION

We have developed a novel and rapid method to decellularize hAM that does not require an operator-dependent mechanical scraping step. This study is the first to compare decellularized hAM with fresh and conventionally preserved hAM. Disruption of the architecture of D-hAM was observed but the integrity of the basement components was preserved. Whatever the treatment used, hAM had no cytotoxic effect, and D-hAM significantly enhanced the metabolic activity of hBMSCs once seeded on D-hAM compared to other treatments. Our method also enhanced the mechanical properties of hAM and prolonged its longevity after implantation, making it an attractive matrix for tissue engineering.

Acknowledgements:

This work contributes to the COST Action CA17116 "*International Network for Translating Research on Perinatal Derivatives into Therapeutic Approaches (SPRINT)*", supported by COST (European Cooperation in Science and Technology). The authors thank Reine Bareille for her help in cell extraction and culture, Laetitia Medan as manager of the animal facility, Patrick Guitton for his technical support, Ray Cooke (professional proof-reader) for copyediting the manuscript, and Aurélie Pagnon (Novotec). We also acknowledge *La Fondation des gueules cassées* for financial support.

FIGURE LEGENDS

Figure 1. Validation of decellularization process

The effectiveness of the decellularization method was assessed according to three previously established criteria [32]. (A) DAPI staining of nuclear material was strong on the non-treated hAM, whereas no fluorescent labeling was observed on D-hAM. This lack of staining showed that the decellularization process completely removed the nuclear material. (B) DAPI staining of histological sections of the four hAMs. The epithelial cells were clearly visible in F-hAM, C-hAM and L-hAM, and few hAMSCs were observed in F-hAM and C-hAM. Scale bar: 50 µm. (C) After extraction, the DNA content of D-hAM was lower than 50 ng/mg of dry tissue. (D) In the decellularized sample, no residual DNA was observed on agarose gel

electrophoresis, whereas in non-treated hAM, the residual DNA ranged from 100 bp to greater than 1500 bp and likely included intact full-length DNA. Data are presented as means + /- standard deviation. The symbol * indicates a statistically significant difference compared to the other group with $p<0.05$).

Figure 2. Influence of preservation methods on morphological aspect and components of hAM.

(A) Light microscopy of amniotic membrane stained using HES. C-hAM closely resembles F-hAM, whereas lyophilization caused compaction of L-hAM and D-hAM. Black asterisks show epithelial layer of hAM. Scale bar: 100 µm. (B) Representative immunohistochemical staining of extracellular matrix and basement membrane components of amniotic membranes. Abbreviations: Coll I, type I collagen; Coll III, type III collagen; Coll IV, type IV collagen; Coll V, type V collagen. Scale bar:50 µm.

Figure 3. Comparison of physical and mechanical properties of fresh and preserved HAM.

(A) Preservation significantly changed the thickness of hAM (n=16). (B) Fresh and decellularized hAM were significantly stronger than C-hAM and L-hAM (n=15 per condition). Fmax: Maximal force before rupture. (C) Decellularization made hAM significantly more stretchable than F-hAM (n=15 per condition). Max Strain: strain at break. (ANOVA; Mean + /- standard deviation. *$p < 0.05$; **$p < 0.01$; *** $p <0.001$).

Figure 4: Extract and contact *in vitro* cytotoxicity of fresh and preserved hAM on human bone marrow stem cells (hBMSCs).

(A) Neutral red assay. Relative cell viability expressed as a percentage of untreated blank. Soluble extracts of cryopreserved hAM (C-hAM) significantly reduced hBMSCs cell viability after one day (E1) compared to F-hAM, L-hAM and D-hAM. No statistical difference in hBMSCs cell viability was observed with soluble extracts collected at day 2 and 3 (E2-E3) (n=12 per condition; ANOVA, *** $p <0.001$). (B) MTT assay. Relative metabolic activity expressed as percentage of untreated blank. The decrease in number of living cells due to soluble extract of C-hAM at day 1 (E1) resulted in a significant decrease in metabolic activity. However, the relative cell viability and metabolic activity of hBMSCs were higher than 70 % of the control group, demonstrating the non-cytotoxic effect of soluble extract of fresh and preserved hAM. (n=12; ANOVA, *$p < 0.05$; **$p < 0.01$; *** $p <0.001$). (C) Relative metabolic activity of hBMSCs seeded on fresh and preserved hAM. Data were normalized to positive control that represented 100% metabolic activity at day 1. Their metabolic activity was significantly enhanced when hBMSCs were seeded on decellularized hAM (D-hAM)

compared to control. (n= 9 per condition; ANOVA, * Indicates a statistically significant difference compared to control, *p < 0.05; **p < 0.01; *** p <0.001). Results are expressed as: mean + /- standard deviation.

Figure 5. Implantation of hAM patches in rat subcutaneous model

(A) Macroscopic appearance of fresh and preserved hAM implants. (B) Implantation procedure. (C) and (D) Surgery and suture of hAM patches.

Figure 6. Resorption of hAM after subcutaneous implantation in rats

(A) Representative histological and immunofluorescence (IF) staining of explanted fresh and preserved hAM and suture control. Black and white asterisks show residual hAM and black arrows indicate non-absorbable suture. Scale bar histological analysis: 2.5mm; Scale bar IF: 250µm. (B) Resorption rate of fresh and preserved hAM was measured using HES staining. D-hAM had the slowest rate of resorption. (n= 9 samples per condition at one week, n=10 samples at one and two months; ANOVA; *p < 0.05; **p < 0.01; *** p <0.001).

Figure 7. Biocompatibility of fresh and preserved hAM

(A) Representative histological sections stained with HES after subcutaneous implantation. At one week, F-hAM and C-hAM exhibited higher host-cell infiltration. Black asterisks show residual hAM (Scale bar: 50µm). (B) Histological sections were evaluated and scored according to NF-EN-ISO 10993-6 standard. The test samples were considered as non-irritant (N: up to 2.9), slightly (S: 3.0 up to 8.9) to moderately irritant (M: 9.0 up to 15.0) and severely irritant (> 15) to tissue as compared to sham-operated control sample (n= 9 samples per condition at one week, n=10 samples at one and two months).

Supplementary Table S1. Antibodies used for immunohistochemical analysis

BIBLIOGRAPHY

[1] Mamede AC, Carvalho MJ, Abrantes AM, Laranjo M, Maia CJ, Botelho MF. Amniotic membrane: from structure and functions to clinical applications. Cell Tissue Res 2012;349:447–58. doi:10.1007/s00441-012-1424-6.

[2] Bourne G. The foetal membranes. A review of the anatomy of normal amnion and chorion and some aspects of their function. Postgrad Med J 1962;38:193–201.

[3] Fukuda K, Chikama T, Nakamura M, Nishida T. Differential distribution of subchains of the basement membrane components type IV collagen and laminin among the amniotic membrane, cornea, and conjunctiva. Cornea 1999;18:73–9.

[4] Niknejad H, Peirovi H, Jorjani M, Ahmadiani A, Ghanavi J, Seifalian AM. Properties of the amniotic membrane for potential use in tissue engineering. Eur Cell Mater 2008;15:88–99.

[5] Malhotra C, Jain AK. Human amniotic membrane transplantation: Different modalities of its use in ophthalmology. World J Transplant 2014;4:111–21. doi:10.5500/wjt.v4.i2.111.

[6] Jirsova K, Jones GLA. Amniotic membrane in ophthalmology: properties, preparation, storage and indications for grafting-a review. Cell Tissue Bank 2017;18:193–204. doi:10.1007/s10561-017-9618-5.

[7] Ilic D, Vicovac L, Nikolic M, Lazic Ilic E. Human amniotic membrane grafts in therapy of chronic non-healing wounds. Br Med Bull 2016;117:59–67. doi:10.1093/bmb/ldv053.

[8] Nguyen KN, Bobba S, Richardson A, Park M, Watson SL, Wakefield D, et al. Native and synthetic scaffolds for limbal epithelial stem cell transplantation. Acta Biomater 2018;65:21–35. doi:10.1016/j.actbio.2017.10.037.

[9] Kubo M, Sonoda Y, Muramatsu R, Usui M. Immunogenicity of human amniotic membrane in experimental xenotransplantation. Invest Ophthalmol Vis Sci 2001;42:1539–46.

[10] Kang JW, Koo HC, Hwang SY, Kang SK, Ra JC, Lee MH, et al. Immunomodulatory effects of human amniotic membrane-derived mesenchymal stem cells. J Vet Sci 2012;13:23–31.

[11] Runic R, Lockwood CJ, Ma Y, Dipasquale B, Guller S. Expression of Fas ligand by human cytotrophoblasts: implications in placentation and fetal survival. J Clin Endocrinol Metab 1996;81:3119–22. doi:10.1210/jcem.81.8.8768884.

[12] Hao Y, Ma DH, Hwang DG, Kim WS, Zhang F. Identification of antiangiogenic and

antiinflammatory proteins in human amniotic membrane. Cornea 2000;19:348–52.

[13] Lee SB, Li DQ, Tan DT, Meller DC, Tseng SC. Suppression of TGF-beta signaling in both normal conjunctival fibroblasts and pterygial body fibroblasts by amniotic membrane. Curr Eye Res 2000;20:325–34.

[14] Ricci E, Vanosi G, Lindenmair A, Hennerbichler S, Peterbauer-Scherb A, Wolbank S, et al. Anti-fibrotic effects of fresh and cryopreserved human amniotic membrane in a rat liver fibrosis model. Cell Tissue Bank 2013;14:475–88. doi:10.1007/s10561-012-9337-x.

[15] Lemke A, Ferguson J, Gross K, Penzenstadler C, Bradl M, Mayer RL, et al. Transplantation of human amnion prevents recurring adhesions and ameliorates fibrosis in a rat model of sciatic nerve scarring. Acta Biomater 2018;66:335–49. doi:10.1016/j.actbio.2017.11.042.

[16] Song M, Wang W, Ye Q, Bu S, Shen Z, Zhu Y. The repairing of full-thickness skin deficiency and its biological mechanism using decellularized human amniotic membrane as the wound dressing. Mater Sci Eng C Mater Biol Appl 2017;77:739–47. doi:10.1016/j.msec.2017.03.232.

[17] Yang L, Shirakata Y, Shudou M, Dai X, Tokumaru S, Hirakawa S, et al. New skin-equivalent model from de-epithelialized amnion membrane. Cell Tissue Res 2006;326:69–77. doi:10.1007/s00441-006-0208-2.

[18] Díaz-Prado S, Rendal-Vázquez ME, Muiños-López E, Hermida-Gómez T, Rodríguez-Cabarcos M, Fuentes-Boquete I, et al. Potential use of the human amniotic membrane as a scaffold in human articular cartilage repair. Cell Tissue Bank 2010;11:183–95. doi:10.1007/s10561-009-9144-1.

[19] Shortt AJ, Secker GA, Lomas RJ, Wilshaw SP, Kearney JN, Tuft SJ, et al. The effect of amniotic membrane preparation method on its ability to serve as a substrate for the ex-vivo expansion of limbal epithelial cells. Biomaterials 2009;30:1056–65. doi:10.1016/j.biomaterials.2008.10.048.

[20] Amemiya T, Nakamura T, Yamamoto T, Kinoshita S, Kanamura N. Immunohistochemical study of oral epithelial sheets cultured on amniotic membrane for oral mucosal reconstruction. Biomed Mater Eng 2010;20:37–45. doi:10.3233/BME-2010-0613.

[21] Iwasaki K, Komaki M, Yokoyama N, Tanaka Y, Taki A, Honda I, et al. Periodontal regeneration using periodontal ligament stem cell-transferred amnion. Tissue Eng Part A 2014;20:693–704. doi:10.1089/ten.TEA.2013.0017.

[22] Rodríguez-Ares MT, López-Valladares MJ, Touriño R, Vieites B, Gude F, Silva MT, et al. Effects of lyophilization on human amniotic membrane. Acta Ophthalmol (Copenh)

2009;87:396–403. doi:10.1111/j.1755-3768.2008.01261.x.

[23] Niknejad H, Deihim T, Solati-Hashjin M, Peirovi H. The effects of preservation procedures on amniotic membrane's ability to serve as a substrate for cultivation of endothelial cells. Cryobiology 2011;63:145–51. doi:10.1016/j.cryobiol.2011.08.003.

[24] Fénelon M, Catros S, Fricain JC. What is the benefit of using amniotic membrane in oral surgery? A comprehensive review of clinical studies. Clin Oral Investig 2018;22:1881–91. doi:10.1007/s00784-018-2457-3.

[25] Laranjo M. Preservation of Amniotic Membrane. In: Mamede AC, Botelho MF, editors. Amniotic Membr. Orig. Charact. Med. Appl., Dordrecht: Springer Netherlands; 2015, p. 209–30. doi:10.1007/978-94-017-9975-1_13.

[26] Fénelon M, Chassande O, Kalisky J, Gindraux F, Brun S, Bareille R, et al. Human amniotic membrane for guided bone regeneration of calvarial defects in mice. J Mater Sci Mater Med 2018;29:78. doi:10.1007/s10856-018-6086-9.

[27] Chen Y-J, Chung M-C, Jane Yao C-C, Huang C-H, Chang H-H, Jeng J-H, et al. The effects of acellular amniotic membrane matrix on osteogenic differentiation and ERK1/2 signaling in human dental apical papilla cells. Biomaterials 2012;33:455–63. doi:10.1016/j.biomaterials.2011.09.065.

[28] Tang K, Wu J, Xiong Z, Ji Y, Sun T, Guo X. Human acellular amniotic membrane: A potential osteoinductive biomaterial for bone regeneration. J Biomater Appl 2017:885328217739753. doi:10.1177/0885328217739753.

[29] Gholipourmalekabadi M, Mozafari M, Salehi M, Seifalian A, Bandehpour M, Ghanbarian H, et al. Development of a Cost-Effective and Simple Protocol for Decellularization and Preservation of Human Amniotic Membrane as a Soft Tissue Replacement and Delivery System for Bone Marrow Stromal Cells. Adv Healthc Mater 2015;4:918–26. doi:10.1002/adhm.201400704.

[30] Zhang T, Yam GH-F, Riau AK, Poh R, Allen JC, Peh GS, et al. The effect of amniotic membrane de-epithelialization method on its biological properties and ability to promote limbal epithelial cell culture. Invest Ophthalmol Vis Sci 2013;54:3072–81. doi:10.1167/iovs.12-10805.

[31] Gholipourmalekabadi M, Bandehpour M, Mozafari M, Hashemi A, Ghanbarian H, Sameni M, et al. Decellularized human amniotic membrane: more is needed for an efficient dressing for protection of burns against antibiotic-resistant bacteria isolated from burn patients. Burns J Int Soc Burn Inj 2015;41:1488–97. doi:10.1016/j.burns.2015.04.015.

[32] Crapo PM, Gilbert TW, Badylak SF. An overview of tissue and whole organ

decellularization processes. Biomaterials 2011;32:3233–43. doi:10.1016/j.biomaterials.2011.01.057.

[33] Hopkinson A, Shanmuganathan VA, Gray T, Yeung AM, Lowe J, James DK, et al. Optimization of amniotic membrane (AM) denuding for tissue engineering. Tissue Eng Part C Methods 2008;14:371–81. doi:10.1089/ten.tec.2008.0315.

[34] Wilshaw S-P, Kearney J, Fisher J, Ingham E. Biocompatibility and potential of acellular human amniotic membrane to support the attachment and proliferation of allogeneic cells. Tissue Eng Part A 2008;14:463–72. doi:10.1089/tea.2007.0145.

[35] Amensag S, McFetridge PS. Rolling the human amnion to engineer laminated vascular tissues. Tissue Eng Part C Methods 2012;18:903–12. doi:10.1089/ten.TEC.2012.0119.

[36] Swim MM, Albertario A, Iacobazzi D, Caputo M, Ghorbel MT. Amnion-based scaffold with enhanced strength and biocompatibility for in vivo vascular repair. Tissue Eng Part A 2018. doi:10.1089/ten.TEA.2018.0175.

[37] Wilshaw S-P, Kearney JN, Fisher J, Ingham E. Production of an acellular amniotic membrane matrix for use in tissue engineering. Tissue Eng 2006;12:2117–29. doi:10.1089/ten.2006.12.2117.

[38] Figueiredo GS, Bojic S, Rooney P, Wilshaw S-P, Connon CJ, Gouveia RM, et al. Gamma-irradiated human amniotic membrane decellularised with sodium dodecyl sulfate is a more efficient substrate for the ex vivo expansion of limbal stem cells. Acta Biomater 2017;61:124–33. doi:10.1016/j.actbio.2017.07.041.

[39] Von Versen-Hoeynck F, Steinfeld AP, Becker J, Hermel M, Rath W, Hesselbarth U. Sterilization and preservation influence the biophysical properties of human amnion grafts. Biol J Int Assoc Biol Stand 2008;36:248–55. doi:10.1016/j.biologicals.2008.02.001.

[40] Lim LS, Poh RWY, Riau AK, Beuerman RW, Tan D, Mehta JS. Biological and ultrastructural properties of acelagraft, a freeze-dried γ-irradiated human amniotic membrane. Arch Ophthalmol Chic Ill 1960 2010;128:1303–10. doi:10.1001/archophthalmol.2010.222.

[41] Wolbank S, Hildner F, Redl H, van Griensven M, Gabriel C, Hennerbichler S. Impact of human amniotic membrane preparation on release of angiogenic factors. J Tissue Eng Regen Med 2009;3:651–4. doi:10.1002/term.207.

[42] Nakamura T, Sekiyama E, Takaoka M, Bentley AJ, Yokoi N, Fullwood NJ, et al. The use of trehalose-treated freeze-dried amniotic membrane for ocular surface reconstruction. Biomaterials 2008;29:3729–37. doi:10.1016/j.biomaterials.2008.05.023.

[43] Vilamitjana-Amedee J, Bareille R, Rouais F, Caplan AI, Harmand MF. Human bone marrow stromal cells express an osteoblastic phenotype in culture. In Vitro Cell Dev Biol

Anim 1993;29A:699–707.

[44] O'Brien J, Wilson I, Orton T, Pognan F. Investigation of the Alamar Blue (resazurin) fluorescent dye for the assessment of mammalian cell cytotoxicity. Eur J Biochem 2000;267:5421–6.

[45] Oliveira H, Catros S, Boiziau C, Siadous R, Marti-Munoz J, Bareille R, et al. The proangiogenic potential of a novel calcium releasing biomaterial: Impact on cell recruitment. Acta Biomater 2016;29:435–45. doi:10.1016/j.actbio.2015.10.003.

[46] Ryzhuk V, Zeng X-X, Wang X, Melnychuk V, Lankford L, Farmer D, et al. Human amnion extracellular matrix derived bioactive hydrogel for cell delivery and tissue engineering. Mater Sci Eng C Mater Biol Appl 2018;85:191–202. doi:10.1016/j.msec.2017.12.026.

[47] Yang B, Zhang Y, Zhou L, Sun Z, Zheng J, Chen Y, et al. Development of a porcine bladder acellular matrix with well-preserved extracellular bioactive factors for tissue engineering. Tissue Eng Part C Methods 2010;16:1201–11. doi:10.1089/ten.TEC.2009.0311.

[48] Dahl SLM, Kypson AP, Lawson JH, Blum JL, Strader JT, Li Y, et al. Readily available tissue-engineered vascular grafts. Sci Transl Med 2011;3:68ra9. doi:10.1126/scitranslmed.3001426.

[49] Luc G, Charles G, Gronnier C, Cabau M, Kalisky C, Meulle M, et al. Decellularized and matured esophageal scaffold for circumferential esophagus replacement: Proof of concept in a pig model. Biomaterials 2018;175:1–18. doi:10.1016/j.biomaterials.2018.05.023.

[50] Riau AK, Beuerman RW, Lim LS, Mehta JS. Preservation, sterilization and de-epithelialization of human amniotic membrane for use in ocular surface reconstruction. Biomaterials 2010;31:216–25. doi:10.1016/j.biomaterials.2009.09.034.

[51] Fairbairn NG, Randolph MA, Redmond RW. The clinical applications of human amnion in plastic surgery. J Plast Reconstr Aesthetic Surg JPRAS 2014;67:662–75. doi:10.1016/j.bjps.2014.01.031.

[52] Gindraux F, Laurent R, Nicod L, de Billy B, Meyer C, Zwetyenga N, et al. Human amniotic membrane: clinical uses, patents and marketed products. Recent Pat Regen Med 2013;3:193–214.

[53] Sanluis-Verdes A, Yebra-Pimentel Vilar MT, García-Barreiro JJ, García-Camba M, Ibáñez JS, Doménech N, et al. Production of an acellular matrix from amniotic membrane for the synthesis of a human skin equivalent. Cell Tissue Bank 2015;16:411–23. doi:10.1007/s10561-014-9485-2.

[54] Chuck RS, Graff JM, Bryant MR, Sweet PM. Biomechanical characterization of

human amniotic membrane preparations for ocular surface reconstruction. Ophthalmic Res 2004;36:341–8. doi:10.1159/000081637.

[55] Jabareen M, Mallik AS, Bilic G, Zisch AH, Mazza E. Relation between mechanical properties and microstructure of human fetal membranes: an attempt towards a quantitative analysis. Eur J Obstet Gynecol Reprod Biol 2009;144 Suppl 1:S134-141. doi:10.1016/j.ejogrb.2009.02.032.

[56] Li W, Ma G, Brazile B, Li N, Dai W, Butler JR, et al. Investigating the Potential of Amnion-Based Scaffolds as a Barrier Membrane for Guided Bone Regeneration. Langmuir ACS J Surf Colloids 2015;31:8642–53. doi:10.1021/acs.langmuir.5b02362.

[57] Shi P, Gao M, Shen Q, Hou L, Zhu Y, Wang J. Biocompatible surgical meshes based on decellularized human amniotic membrane. Mater Sci Eng C Mater Biol Appl 2015;54:112–9. doi:10.1016/j.msec.2015.05.008.

[58] Allen CL, Clare G, Stewart EA, Branch MJ, McIntosh OD, Dadhwal M, et al. Augmented dried versus cryopreserved amniotic membrane as an ocular surface dressing. PloS One 2013;8:e78441. doi:10.1371/journal.pone.0078441.

[59] Wiebe JP, Dinsdale CJ. Inhibition of cell proliferation by glycerol. Life Sci 1991;48:1511–7.

[60] Sugiyama N, Mizuguchi T, Aoki T, Hui T, Inderbitzin D, Demetriou AA, et al. Glycerol suppresses proliferation of rat hepatocytes and human HepG2 cells. J Surg Res 2002;103:236–42. doi:10.1006/jsre.2002.6367.

[61] Sieme H, Oldenhof H, Wolkers WF. Mode of action of cryoprotectants for sperm preservation. Anim Reprod Sci 2016;169:2–5. doi:10.1016/j.anireprosci.2016.02.004.

[62] Salah RA, Mohamed IK, El-Badri N. Development of decellularized amniotic membrane as a bioscaffold for bone marrow-derived mesenchymal stem cells: ultrastructural study. J Mol Histol 2018. doi:10.1007/s10735-018-9768-1.

[63] Kesting MR, Wolff K-D, Mücke T, Demtroeder C, Kreutzer K, Schulte M, et al. A bioartificial surgical patch from multilayered human amniotic membrane-In vivo investigations in a rat model. J Biomed Mater Res B Appl Biomater 2009;90:930–8. doi:10.1002/jbm.b.31365.

[64] Ilancheran S, Moodley Y, Manuelpillai U. Human fetal membranes: a source of stem cells for tissue regeneration and repair? Placenta 2009;30:2–10. doi:10.1016/j.placenta.2008.09.009.

[65] Litwiniuk M, Radowicka M, Krejner A, Śladowska A, Grzela T. Amount and distribution of selected biologically active factors in amniotic membrane depends on the part

of amnion and mode of childbirth. Can we predict properties of amnion dressing? A proof-of-concept study. Cent-Eur J Immunol 2018;43:97–102. doi:10.5114/ceji.2017.69632.

[66] López-Valladares MJ, Teresa Rodríguez-Ares M, Touriño R, Gude F, Teresa Silva M, Couceiro J. Donor age and gestational age influence on growth factor levels in human amniotic membrane. Acta Ophthalmol (Copenh) 2010;88:e211-216. doi:10.1111/j.1755-3768.2010.01908.x.

A.

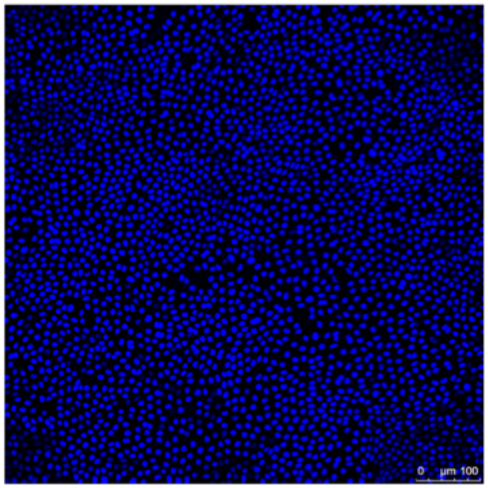

Non treated hAM

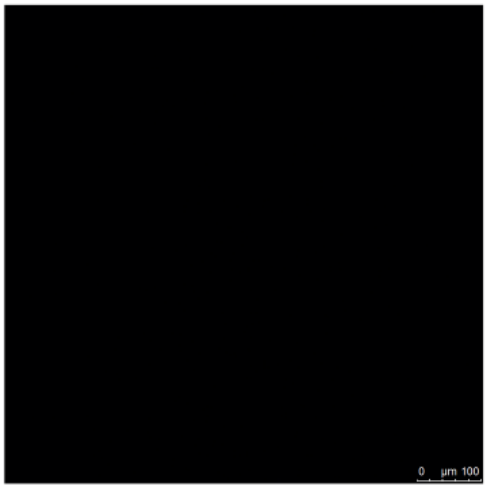

D-hAM

B.

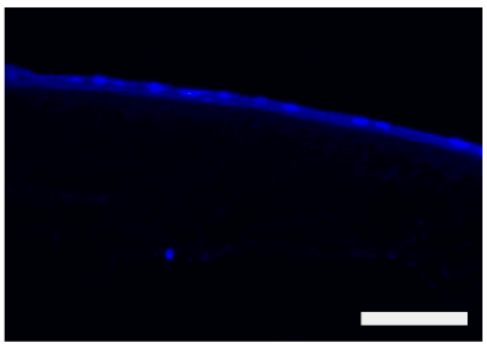

F-hAM

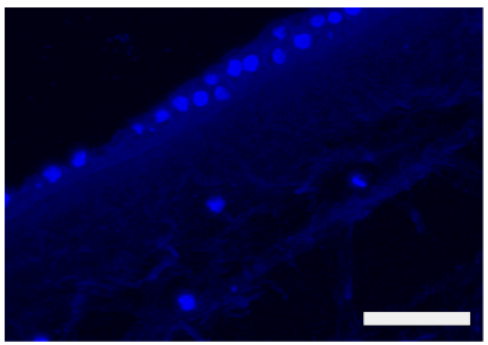

C-hAM

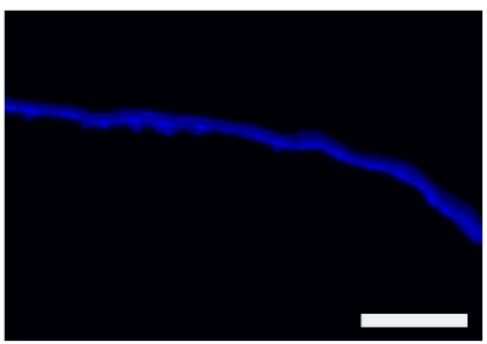

L-hAM

D-hAM

C.

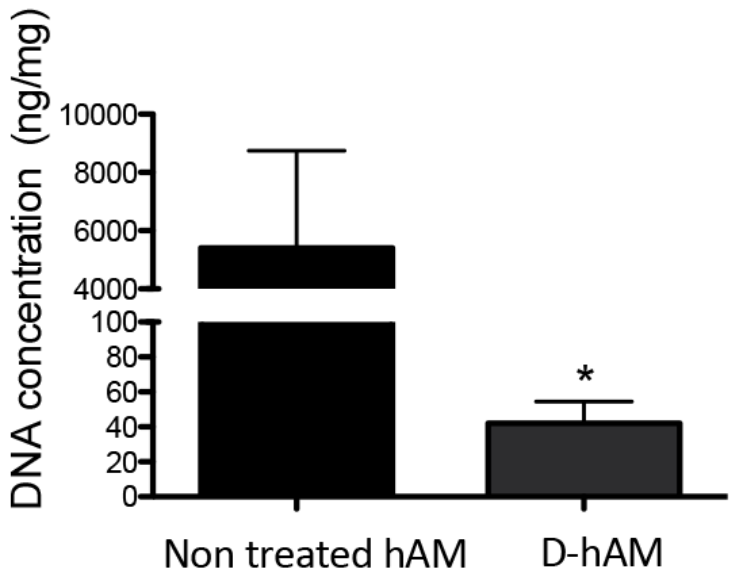

D.

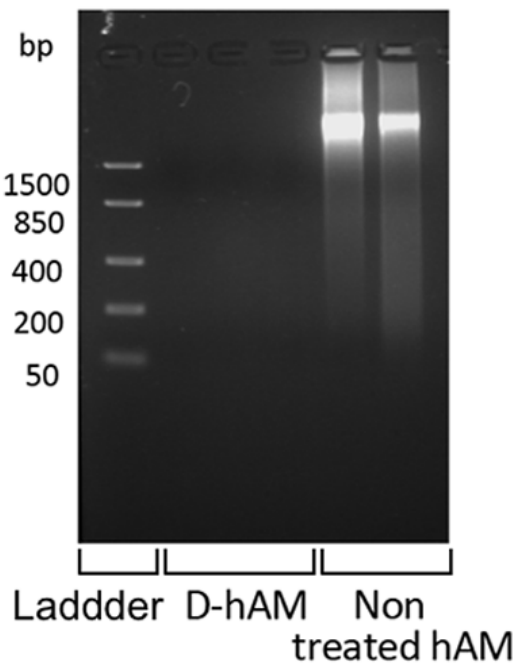

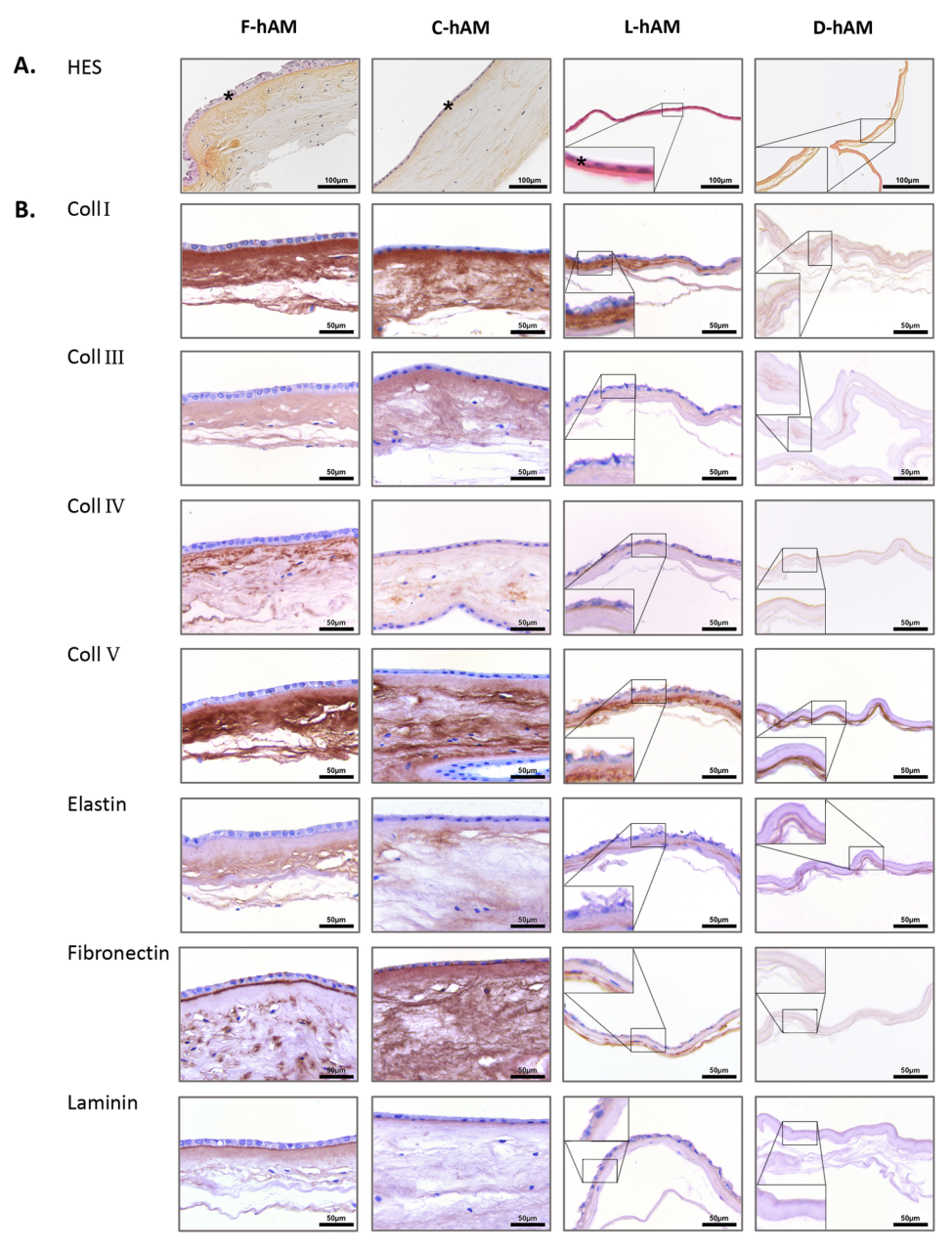
F-hAM
C-hAM
L-hAM
D-hAM
A.
HES
B.
Coll I
Coll III
Coll IV
Coll V
Elastin
Fibronectin
Laminin
100μm
50μm

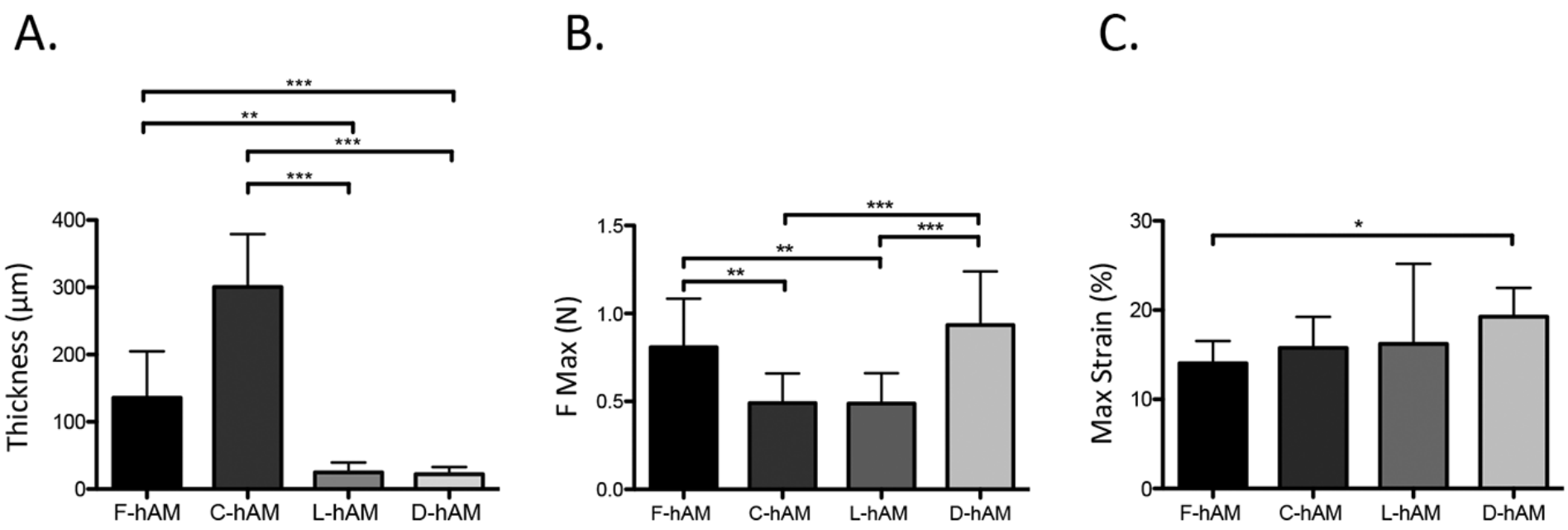
A.
B.
C.
Thickness (µm)
F Max (N)
Max Strain (%)
F-hAM
C-hAM
L-hAM
D-hAM
***
**
*

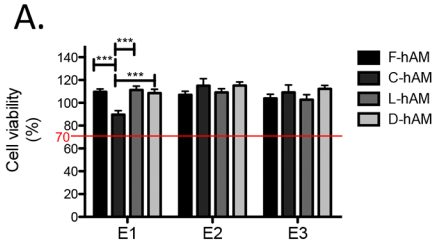
A.
Cell viability (%)
140
120
100
80
70
60
40
20
0
E1
E2
E3
F-hAM
C-hAM
L-hAM
D-hAM

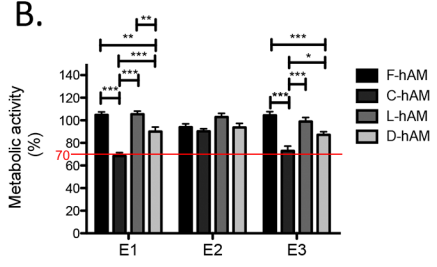
B.
Metabolic activity (%)
140
120
100
80
70
60
40
20
0
E1
E2
E3
F-hAM
C-hAM
L-hAM
D-hAM

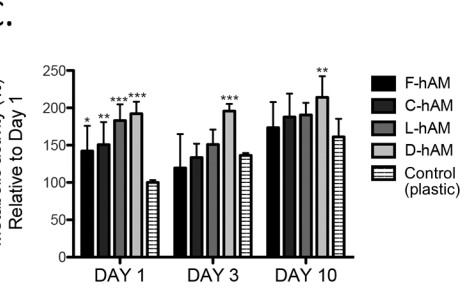
C.
Metabolic activity (%)
Relative to Day 1
250
200
150
100
50
0
DAY 1
DAY 3
DAY 10
F-hAM
C-hAM
L-hAM
D-hAM
Control
(plastic)

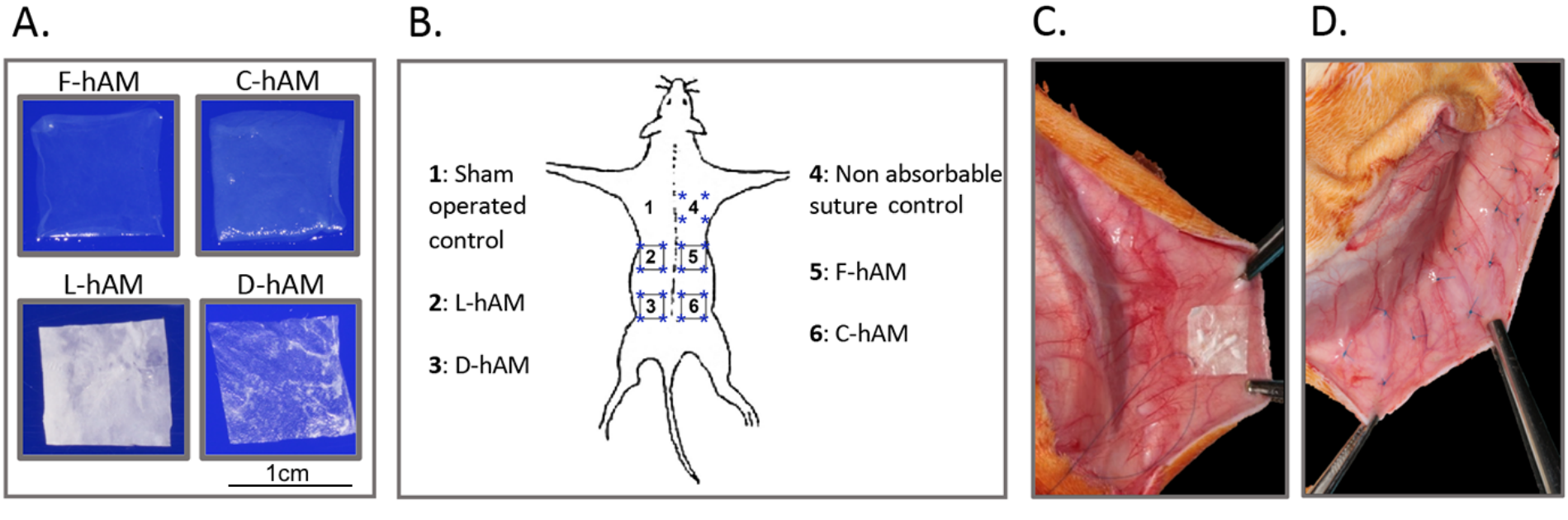
A.
F-hAM
C-hAM
L-hAM
D-hAM
1cm
B.
1: Sham operated control
2: L-hAM
3: D-hAM
4: Non absorbable suture control
5: F-hAM
6: C-hAM
1
2
3
4
5
6
C.
D.

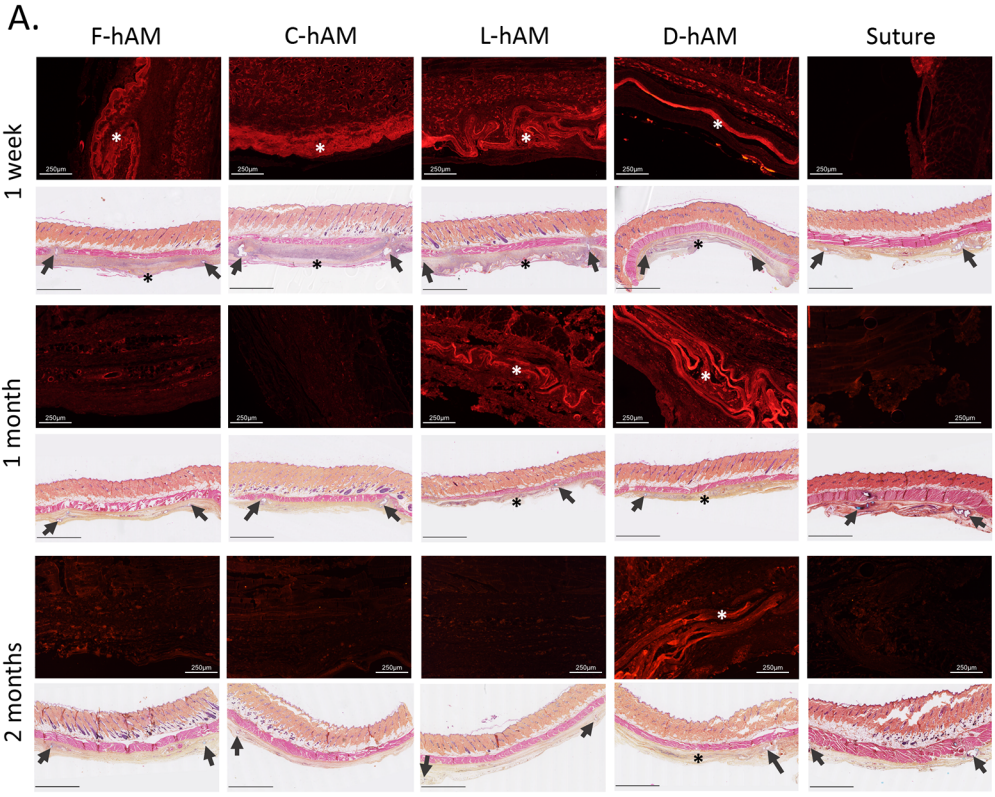
A.
F-hAM
C-hAM
L-hAM
D-hAM
Suture
1 week
1 month
2 months
250μm

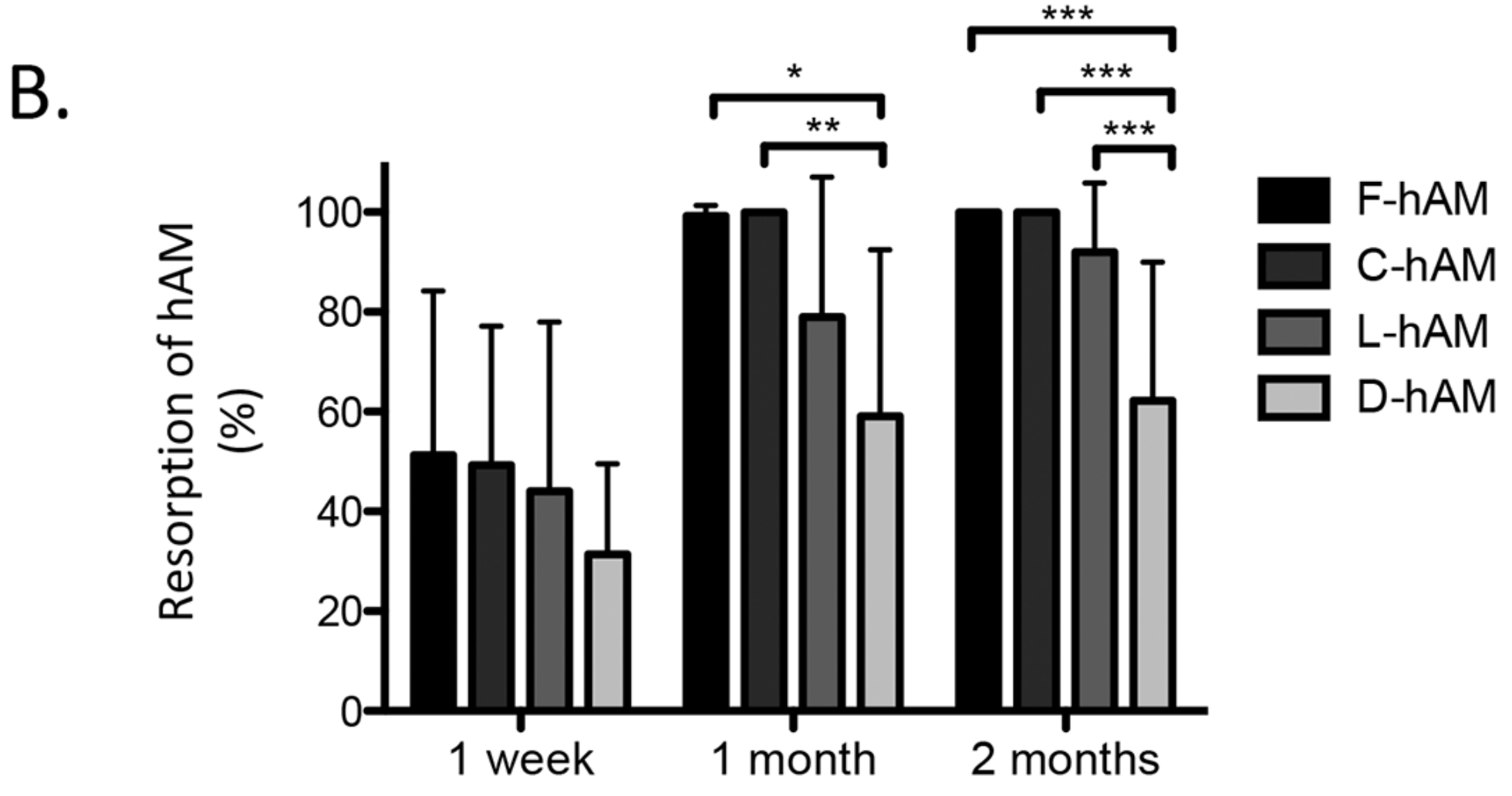
B.
Resorption of hAM (%)
100
80
60
40
20
0
1 week
1 month
2 months
*
**
***
***
***
F-hAM
C-hAM
L-hAM
D-hAM

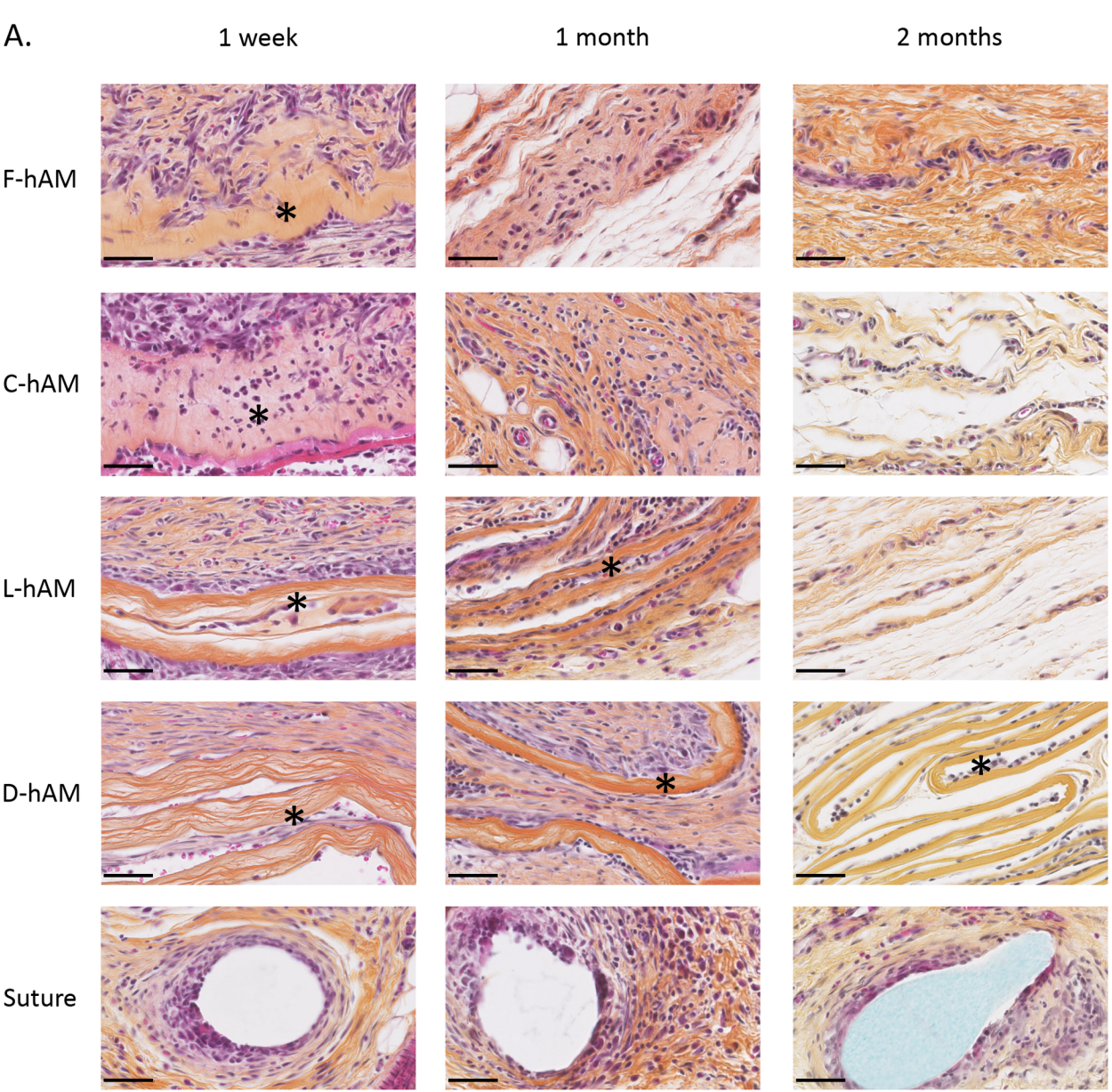
A.
1 week
1 month
2 months
F-hAM
C-hAM
L-hAM
D-hAM
Suture

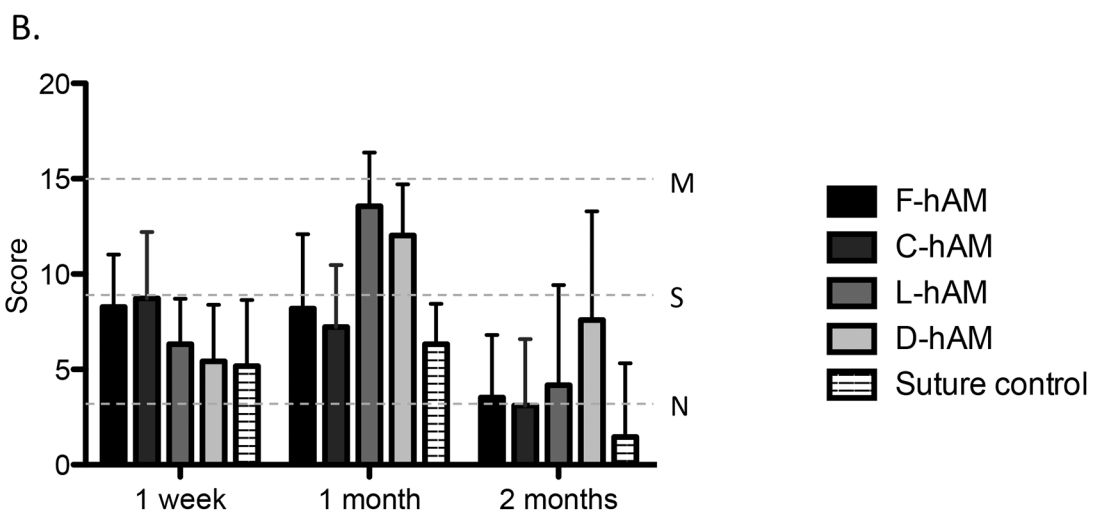
B.
20
15
10
5
0
Score
M
S
N
1 week
1 month
2 months
F-hAM
C-hAM
L-hAM
D-hAM
Suture control

Antibody	Reference and batch	Dilution
Rabbit anti-human Type I collagen	Novotec 20111, 380j	1/2000
Mouse anti-human Type III collagen	Novotec 60315, 316f	1/2000
Mouse anti-human Type IV collagen	Novotec 60415, 319n	1/16 000
Rabbit anti-human Type V collagen	Novotec 20511, 317m	1/1000
Rabbit anti-human Elastin	Novotec 25011, 297s	1/2000
Rabbit anti-human Laminin	Novotec 24811, 356c	1/1000
Rabbit anti-human Fibronectin	Novotec 24911, 351k	1/1000

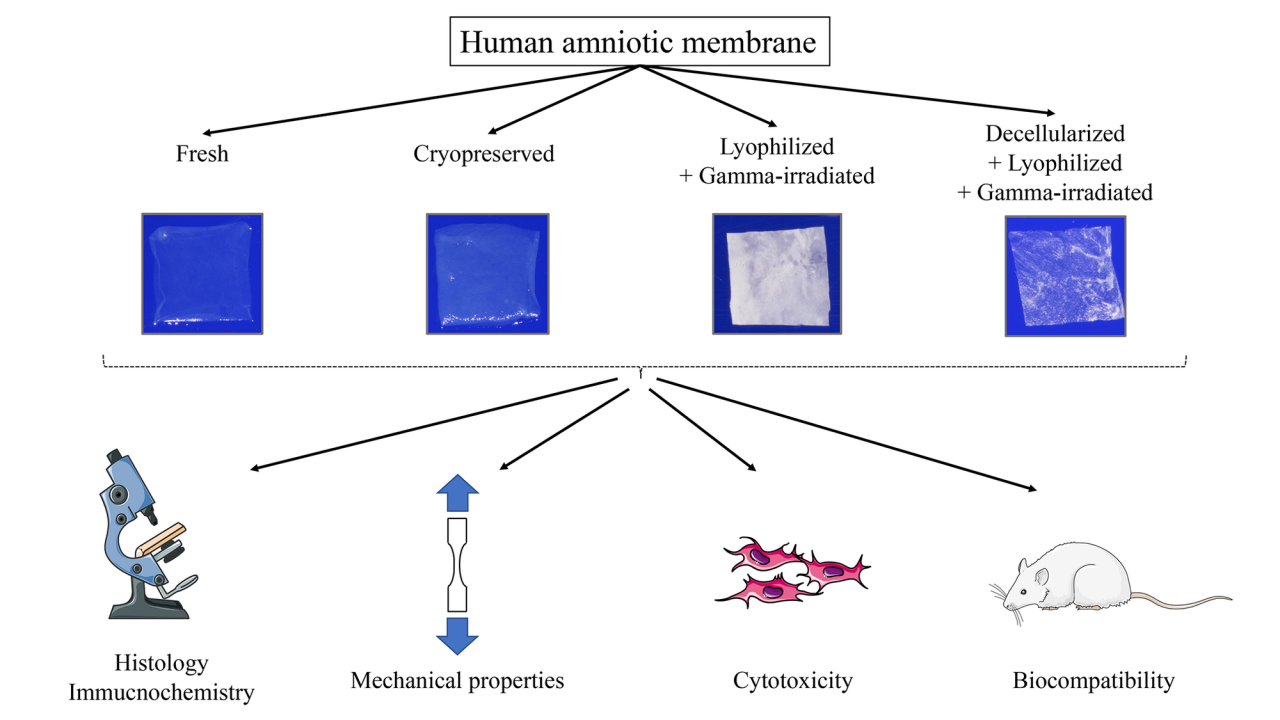
Human amniotic membrane
Fresh
Cryopreserved
Lyophilized
+ Gamma-irradiated
Decellularized
+ Lyophilized
+ Gamma-irradiated
Histology
Immucnochemistry
Mechanical properties
Cytotoxicity
Biocompatibility